Time shift between precipitation and evaporation has more impact on annual streamflow variability than evaporation~~How does the time shift between precipitation and evaporation affect annual streamflow variability? A large sample elasticity study~~

a mis en forme : Non Surlignage

Vazken Andréassian[*,1], Guilherme Mendoza Guimarães[1], Alban de Lavenne[1], Julien Lerat[2]

a mis en forme : Français (France)

[1] Université Paris-Saclay, INRAE, HYCAR Research Unit, Antony, France

[2] CSIRO, Canberra, Australia

[*]Corresponding author : Vazken Andréassian, vazken.andreassian@inrae.fr

Abstract

One of the most basic questions asked ~~to~~ of hydrologists is ~~that of the quantification of catchment response to climatic variations, i.e. that of the variations around the average annual flow given the climatic anomaly of a given~~the quantification of catchment response to climatic variations, i.e., the variations around the average annual flow given the climatic anomaly of a particular year. This paper presents ~~a large sample~~an analysis based on 4122 catchments from four continents, where we investigate how annual streamflow variability depends on climate variables – rainfall and potential evaporation – and on ~~the season when precipitation occurs, i.e. on~~ the synchronicity between precipitation and potential evaporation. We use catchment data to verify the existence of this link~~,~~ and show that, in all countries and under the main climates represented, ~~synchronicity~~ anomalies in this synchronicity ~~come as~~are the second most important factor to explain annual streamflow anomalies,~~:~~ after precipitation, ~~-~~but before potential evaporation. Introducing the synchronicity between precipitation and potential evaporation as an independent variable improves the prediction of annual streamflow variability with an average additional explained variance of 6 % globally ~~significantly~~.

Keywords: annual streamflow anomalies, elasticity, sensitivity, seasonality

Notations

We deal in this paper with three hydrological fluxes: precipitation (P_n), streamflow (Q_n) and potential evaporation (E_{0n}). The three fluxes are computed at catchment scale, expressed in millimeters per year, and represent annual ~~sums~~ totals (index n refers to the year in question). We use a hydrological year from October 1st of year $n-1$ to September 30th of year n in the Northern hemisphere and from April 1st of year n to March 31st of year $n+1$ in the Southern hemisphere. Anomalies (of P, Q and E_0), noted Δ, are computed as the difference between the annual value and the long-term average value, ~~i.e.~~ i.e., $\Delta Q_n = Q_n - \bar{Q}$, $\Delta P_n = P_n - \bar{P}$, etc.

1 Introduction

1.1 On the climate elasticity of streamflow

To assess the impact of climate change on water resources, hydrologists ~~need~~ aim to quantify the ~~response~~ amount of change in catchment flow when ~~with respect to variations in~~ climatic conditions vary. The ratio between changes in streamflow and climate is formally defined as ~~For this, they estimate~~ the climate elasticity of streamflow (Schaake and Liu, 1989). The hydrological literature and ~~hydrologic~~ common sense both suggest that the best factor explaining ~~predictor of~~ the changes in annual streamflow ~~anomaly~~ is the annual precipitation anomaly (~~e.g.~~ e.g., Pardé, 1933a; Leopold, 1974). In addition, many elasticity studies have also considered the anomaly of potential evaporation, although it is usually only weakly statistically significant in regression studies. In this paper, we focus on a third explanatory variable that quantifies ~~quantifying~~ the synchronicity between precipitation and potential evaporation within the year.

1.2 Linear models to predict streamflow anomalies

There is ~~an abundant literature concerning elasticity studies in hydrology, and our work comes in the continuation of~~ continues ~~the earlier empirical (i.e., measurement-based) studies of Sankarasubramanian et al. (2001), Chiew (2006)~~ an abundance of literature concerning elasticity studies in hydrology, and our work builds upon the earlier empirical (i.e., measurement-based) studies of Sankarasubramanian et al. (2001), Chiew (2006), and Andréassian et al. (2016). Here, we follow the same principle and use linear regression models based on measured annual data to evaluate the climate elasticity of streamflow. An alternative approach to ~~estimate climate elasticities would consist in using hydrological models of various~~estimating climate elasticities would involve using hydrological models of varying complexities (e.g.~~,~~ Koster and Suarez, 1999). However, even if models are powerful investigative tools, they also rely on restrictive assumptions that often limit their credibility outside ~~of a~~their calibration range. This can be particularly problematic in a large-scale study on the impact of climate change. Thus, we favo~~u~~red an approach introducing the minimal number of hydrological assumptions, hence a linear regression that also has the advantage ~~to be~~of being ~~conceptually~~ mathematically extremely simple.

1.3 The synchronicity between precipitation and potential evaporation impacts annual streamflow totals

The fact that the ~~the synchronicity (i.e. the~~ time shift~~)~~ between precipitation and potential evaporation, hereon referred to as "climatic synchronicity", has a hydrological impact ~~is~~ has been known for a long time, as shown by a few precursors on this topic. For example,~~:~~ in 1933b

Pardé published ~~in 1933b~~ a classic paper dedicated to the average flow of rivers, where he ~~underlines~~ underlined that "for identical values of precipitation and temperature, everything else being equal, the runoff coefficient Q/P will be smaller where the larger part of precipitation falls during the warm season". Similarly,~~;~~

a mis en forme : Normal, Sans numérotation ni puces

Coutagne and de Martonne (1935) discussed formulas for annual streamflow, and underlined that formulas based only on the humidity ratio P/E_0 are deficient, because they fail to account for "the distribution of precipitations between seasons, in particular, in the temperate zone, between the warm and the cold season. Of two years of equal precipitation, the year which will receive the most part in summer will produce the less annual flow". Additional classical studies include~~;~~

Thornthwaite (1948), who proposed to classify climates initially with two indices (one ~~characterising~~characterizing the periods of water surplus and the other the periods of water deficiency), which he subsequently combined into a single index.~~;~~ Also, Turc introduced in 1954 his famous formula for long-term actual evaporation. At the very end of his paper, he wrote that “the most urgent improvement” to his actual evaporation formula should be the introduction of the “distribution of precipitations and of the temperature changes within the year.”

Recent studies have also discussed the impact of climate seasonality on water balance, based on either theoretical or empirical approaches.~~:~~

~~a~~Among the theoretical studies, ~~one can cite~~ Dooge (1992) ~~who~~ presented catchment yield curves where he introduced as a parameter the length of the dry season.~~;~~ Milly (1994) ~~who~~ proposed a theoretical computation of actual evaporation based on the seasonality of the aridity index. ~~;~~ Yokoo et al. (2008) ~~who~~ made theoretical computations on the difference between in-phase and out-of-phase regimes of precipitation and potential evapotranspiration~~; as well as~~. Additionally, Roderick and Farquhar (2011), Feng et al. (2012) ~~and~~, Donohue et al. (2012), ~~-~~ Berghuijs et al. (2014) and Jawitz et al. (2022) ~~who~~ all made notable developments. ~~-~~ Among t~~;~~

~~Th~~he empirical ~~study~~ studies, ~~of~~ Potter et al. (2005) quantified the impact of rainfall seasonality on mean annual water balance in Australia. Hickel and Zhang (2006) discussed the antagonistic effects of climate seasonality and soil moisture storage. More recently, de Lavenne and Andréassian (2018) proposed a synchronicity index to ~~characterise~~ characterize the phase difference between precipitation and potential evaporation~~. Finally~~, and Feng et al. (2019) proposed an index of asynchronicity for Mediterranean climates.

1.4 Purpose of the paper

~~2~~ In this paper, we aim to improve the prediction of streamflow elasticity by introducing anomalies in synchronicity between precipitation and potential evaporation as a predictor, alongside variability in rainfall and potential evapotranspiration. Our study is based solely on data analysis, and uses only linear regression models.~~In this paper, we wish to demonstrate exclusively through data analysis~~, ~~that anomalies in the seasonality of rainfall represent the second most important factor explaining annual streamflow anomalies~~, ~~s (after precipitation but before potential evaporation). We also wish to show how introducing the synchronicity between precipitation and potential evaporation as an independent variable improves the prediction of annual streamflow variability.~~

a mis en forme : Retrait : Gauche : 0 cm

a mis en forme : Normal, Sans numérotation ni puces

a mis en forme : Normal

a mis en forme : Couleur de police : Automatique

~~3~~2 Test catchments

~~3.1~~2.1 Origin of the dataset

As presented in Table 1, we use catchments from nine countries to base our analysis on a wide range of climates.

a mis en forme : Anglais (États-Unis)

Table 1. Origin of the catchments used in this paper

Country	Number of catchments selected	Number of catchments available in the original dataset	Dataset	Reference
Australia	546	561	Camels-AUS	Fowler et al. (2024)
Brazil	636	734	Cabra	Almagro et al. (2021)
Denmark	202	304	Camels-DK	Liu et al. (2024)
France	628	654	Camels-FR	Delaigue et al. (2024)
Germany	1094	1555	Camels-DE	Loritz et al. (2024)
Sweden	152	158	Selection by G. Lindström	de Lavenne et al. (2022)
Switzerland	73	331	Camels-CH	Höge et al. (2023)
United Kingdom	136	670	Camels-UK	Coxon et al. (2020)
USA	655	672	Camels-US	Addor et al. (2017)

The total number of catchments is 4122, for a total of 162,005 station-years (the average length of catchment time series is 39 years). We use hydrological years as defined in the Notations section.

~~3.2~~2.2 Catchment selection

The catchments used in this paper ~~are~~ were selected from several datasets indicated in Table 1 and represent approximately 75% of the original catchments. Our catchment selection ~~is~~ was based on ~~(i)~~three criteria: ~~:~~

~~1.~~ record length, catchment memory and regulation degree. First, we only ~~selected: selected~~ catchments ~~have all~~that had more than 20 ~~annual~~ complete hydrological years. Second, we~~values; (ii)~~

~~2. catchment memory:~~ selected catchments that exhibit ~~no or little~~minimal interannual memory ("memory" as defined by ~~as per~~ de Lavenne et al., 2022). This criterion was needed because the equation used here to estimate streamflow elasticity is only hydrologically warranted for ~~those~~ catchments displaying ~~no or little~~minimum interannual memory, thus allowing ~~(we wished to warrant~~ a straightforward computation of ~~the~~ annual elasticity coefficients, based only on annual average values. Finally, ~~only);~~

~~3. (iii) regulations: we removed the~~ catchments ~~that the authors of the datasets~~ identified as significantly regulated by reservoirs were removed. This identification was done by either~~(we either asked~~ asking the datasets authors, or, where the information was available, by setting a limit equal to 10 mm equivalent volume storage in dams).

Code de champ modifié

a mis en forme : Police :Non Gras

a mis en forme : Normal, Sans numérotation ni puces

a mis en forme : Police :Non Gras

a mis en forme : Police :Non Gras

For Switzerland, ~~we considered~~ the list of almost natural catchments published by Muelchi et al. (2022) was utilized.~~.~~

~~3.3~~2.3 Climatic inputs

Where several precipitation products were available in the original dataset, we used the product recommended by dataset authors as being of the best quality, while avoiding precipitation data based exclusively on satellite estimates.

In the original datasets, ~~Because~~ potential evaporation was computed with a variety of different formulas ~~in the different~~(Makkink, Morton, FAO-56, Penman-Monteith ~~datasets~~, Hargreaves, Oudin, etc.). For the sake of homogeneity, we recomputed it (at the daily time step) for all catchments using the formula proposed by Oudin et al. (2005), which requires only extraterrestrial radiation and air temperature ~~only~~. This formula was selected for two reasons: first~~On one hand, this formula~~, it could be computed, given the available data, for all datasets, ~~on the other h~~and it has been widely used worldwide and appears ~~to be~~ appropriate (while of course not perfect) ~~to~~ for describ~~e~~ing ~~the~~ atmospheric evaporative demand.

~~3.4~~2.4 Characteristics of the catchment set

In our dataset, the aridity ~~indices~~ index, computed as E_0/P, ranges from 0.1 to 6.3, with a first quartile ~~equal~~ of ~~to~~ 0.6 and a third quartile ~~equal to~~of 1.0. The mean and the median of the aridity index are~~equal~~ both 0.8. In order to assess the generality of the results, we will discuss them at the country scale and also by climatic classes following the Köppen-Geiger classification (see e.g., Peel et al. 2007 and Table 2~~Table 2Table 2~~). Note that we only give numerical results for~~because we did not consider~~ the climatic zones with ~~less~~ more than 100 catchments~~, the 384 catchments belonging to the less-represented zones are left out of the Koppen~~Köppen-Geiger-based~~Koppen-Geiger based analysis~~.

Table 2. Main climatic zones (in the sense of the Köppen-Geiger classification) represented in our dataset (we ~~only~~ present the zones counting more than 100 catchments)

Köppen-Geiger zone	Name	Number of catchments
Aw	Tropical savanna climate with dry winter	344
Cfa	Temperate climate without dry season with hot summer	364

Cfb	Temperate climate without dry season with warm summer	1746
Csa	Temperate climate with dry and hot summers	196
Dfb	Continental climate without dry season with warm summer	956
Dfc	Continental climate without dry season with cold summer	132

~~Last, we present in~~Finally, Figure 1 presents the 4122 catchments of our dataset ~~in~~ with two variants of the Turc-Budyko non-dimensional graph. On the left-hand graph, each catchment corresponds to one point, ~~whose~~ with coordinates ~~correspond to~~representing the average aridity on the x-axis and 'actual evaporation' yield, computed as ~~((P-Q)/P)~~ $(P-Q)/P$, on the y-axis. On the right-hand graph, each catchment ~~corresponds to one point, whose with coordinates correspond torepresenting the average humidity on the x-axis and~~ is represented by a single point, with coordinates indicating the average humidity on the x-axis and the average streamflow yield, computed as Q/P, ~~(Q/P)~~ on the y-axis.

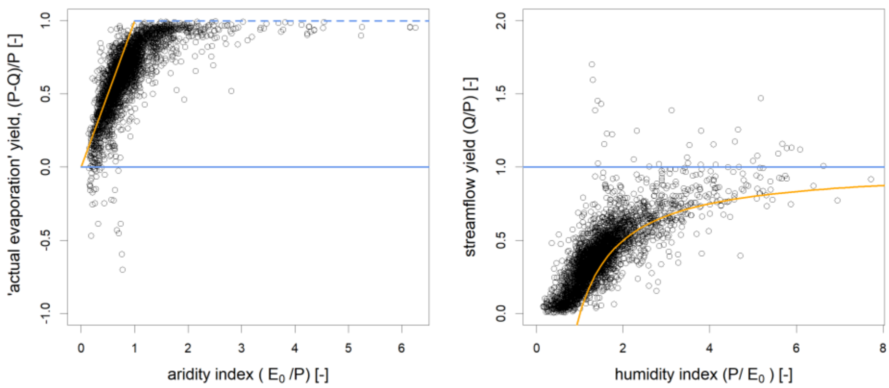

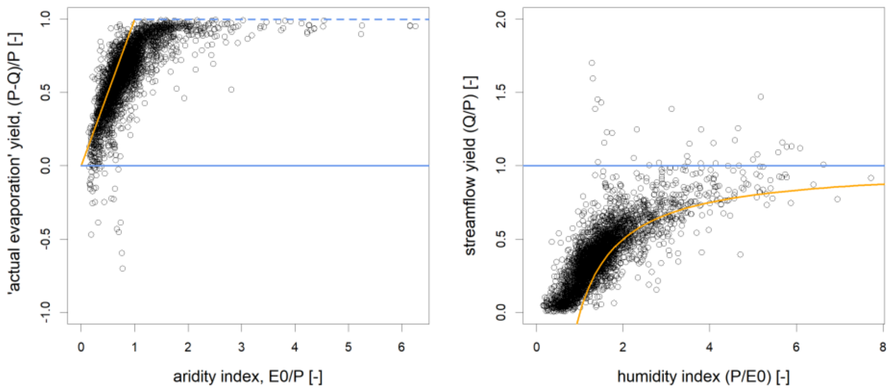

Figure 1: ~~: representation~~Representation of the 4122 catchments in two equivalent forms of the Turc-Budyko non-dimensional space. The solid blue line corresponds to the water limit (Q=P), and the orange line corresponds to the energy limit ($Q=P-E_0$). On the left, an additional limit (dotted blue line) is sometimes improperly referred to as "water limit" in the literature, but it only corresponds to the physical limit (Q=0), when one estimates the actual evaporation as the difference between discharge and precipitation. The catchments that are beyond the orange line (i.e., above on the left and below on the right) are "leaky" (in the sense that they contribute to the recharge of a regional aquifer) and those which are beyond the blue line (i.e., below on the left and above on the right) are "gaining" in the sense of a karstic catchment which would drain a larger than specified catchment (note that~~,~~ in a few cases, data uncertainties might also cause catchments to be beyond the limits).

43 Method

4.13.1 Computation of the synchronicity of precipitation and potential evaporation

In this paper, we useutiliseutilize a modified version of the synchronous precipitationseasonality index λ_n, as in dethat we introduced by (de Lavenne and Andréassian ((, 2018):, and a detailed discussion of the reasons for this change is givenprovided in the Appendix. The objective of this index (Λ) – :in orderis to characterize the synchronicity between precipitation P and potential evapotranspirration E_0 at the annual time stepis measured for each hydrological year n as follows. : For each year *n*, we define the part of annual precipitation that is the most easily accessible to evaporation (i.e., neutralizable by evaporation) as in Eq. 1 and Figure 2:

:

$$\lambda_n \textit{synchronous } P - E_0 \textit{ amount} \textit{easily evaporated precipitation} = \sum_{m=1}^{12} min\left(P_{m,n}, E_{0_{m,n}}\right) \frac{\sum_{m=1}^{12}\left(P_{m,n} \cap E_{0_{m,n}}\right)}{\sum_{m=1}^{12}\left(P_{m,n} \cup E_{0_{m,n}}\right)} \quad \textbf{Eq. 1}$$

where the the index *m* refers to the calendar month and the symbol ∩ denotes the following operation in this paper:.

$$x \cap y = \max(x - y, 0) \quad \text{Eq. 1}$$

a mis en forme : Légende, Pas de paragraphes solidaires

a mis en forme : Justifié, Pas de paragraphes solidaires

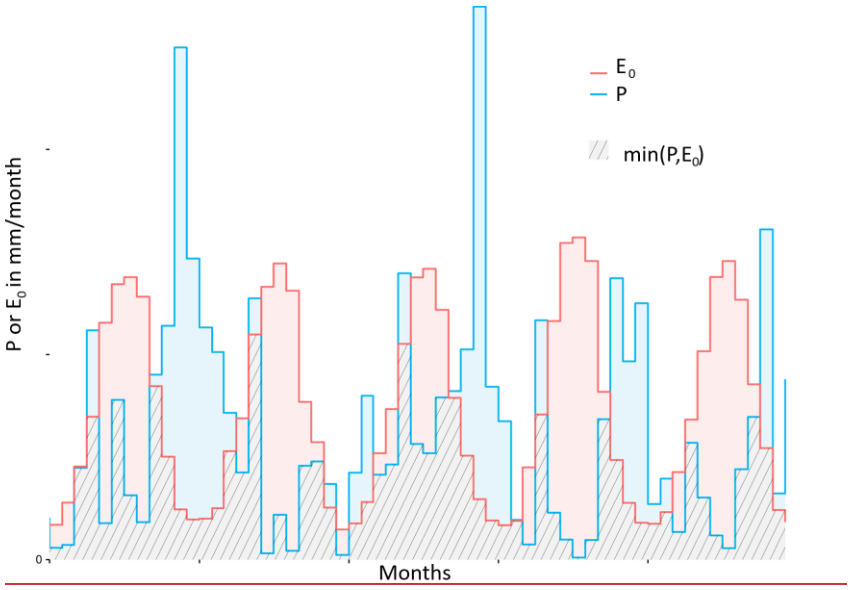

Figure 2. two series of precipitation and potential evaporation at catchment scale: the part of precipitation that is the most easily accessible to evaporation is illustrated in hatched pattern

We define tThe percentage of easily neutralizable precipitation is then defined as Eq. 2, and the percentage of easily neutralizable potential evaporation as that is easily neutralizable asEq. 3.

$$\lambda_{1,n} = \frac{\sum_{m=1}^{12} min\left(P_{m,n}\,, E_{0\,m,n}\right)\left(P_{m,n} \cap E_{0\,m,n}\right)}{P_n} \qquad \text{Eq. 2}$$

and the percentage of potential evaporation that is easily neutralizable as

$$\lambda_{2,n} = \frac{\sum_{m=1}^{12} min\left(P_{m,n}\,, E_{0\,m,n}\right)\left(P_{m,n} \cap E_{0\,m,n}\right)}{E_{0\,n}} \qquad \text{Eq. 3}$$

Because both ratios belong to the interval [0,1], their geometric average will also belong to [0,1]be within the same range (Eq. 4).:

$$\lambda_{3,n} = \sqrt{\lambda_{1,n}\lambda_{2,n}} = \frac{\sum_{m=1}^{12} min\left(P_{m,n}\,, E_{0\,m,n}\right)\left(P_{m,n} \cap E_{0\,m,n}\right)}{\sqrt{P_n * E_{0\,n}}} \qquad \text{Eq. 4}$$

Finally, the index Λ rescales and combines λ_1 and λ_2 into a single quantity, expressed in mm/yr, representing the average ratio of neutralizable precipitation and neutralizable potential evaporation as shown in Eq. 5. For two years with the same annual amounts

a mis en forme : Paragraphes solidaires

a mis en forme : Légende

a mis en forme : Police :

a mis en forme : Police :

a mis en forme : Police :

of precipitation and potential evaporation, Λ will reach higher values when P and E_0 are synchronous, and lower values when they are out of phase.

$$\Lambda_n = \lambda_{3,n} * \bar{P} = \frac{\sum_{m=1}^{12} min\left(P_{m,n}\,, E_{0\,m,n}\right)\left(P_{m,n} \cap E_{0\,m,n}\right)}{\sqrt{P_n * E_{0_n}}} * \bar{P} \qquad \text{Eq. 5}$$

Because λ_n is nondimensional, we then rescale λ_n using the long-term average of the denominator of Eq. 1:

$$\Lambda_n = \lambda_n * \overline{\sum_{m=1}^{12}\left(P_{m,n} \cup E_{0\,m,n}\right)} \qquad \text{Eq. 2}$$

Note that:

- while Λ_n is an annual value, its computation requires the knowledge of the climate forcing at the monthly time step;
- dividing $\sum_{m=1}^{12}\left(P_{m,n} \cap E_{0\,m,n}\right)$ by $\sum_{m=1}^{12}\left(P_{m,n} \cup E_{0\,m,n}\right)$ is a necessity for regression analysis, because we cannot (or at least should not) introduce in a regression independent explanatory variables which are significantly correlated;
- λ_n represents the percentage of annual precipitation that is the most easily accessible to evaporation, and Λ_n (in mm/y) can be interpreted as representing the corresponding annual precipitation amount: for two years with the same annual amounts of precipitation and potential evaporation, Λ will reach higher values when P and E_0 are synchronous, and lower values when they are out of phase.

a mis en forme : Normal, Sans numérotation ni puces

4.23.2 Computation of streamflow elasticities

To compute the streamflow elasticities, we will solve here the two following linear equations given by Eq. 6 and Eq. 7.:

$$\Delta Q_n = e_{Q/P}\Delta P_n + e_{Q/E_0}\Delta E_{0_n} \qquad \text{Eq. 663}$$

$$\Delta Q_n = e_{Q/E_0P}\Delta P_n + e_{Q/E_0}\Delta E_{0_n} + e_{Q/\Lambda}\Delta \Lambda_n \qquad \text{Eq. 774}$$

WWhere ΔVQ_n (respectively ΔP_n, ΔE_{0_n}, $\Delta \Lambda_n$) is represents the deviation from the mean annual value (anomaly) for variable VQ (respectively P, E_0, Λ) (in mm/y) and $e_{Q/VP}$, e_{Q/E_0} and $e_{Q/\Lambda}$ is represent the elasticity of streamflow against with respect to P, E_0, and Λ V (dimensionless).

a mis en forme : Autoriser lignes veuves et orphelines

Eq. 6Eq. 6Eq. 3 represents the classical approach to elasticity computation (see e.g. Andréassian et al., 2016), while. Eq. 7Eq. 7Eq. 4 represents the original contribution of this paper, and aims at determining how far climatic synchronicity explains annual streamflow variability.

Note that:

- the estimation ofThe elasticities in Eq. 6Eq. 6Eq. 3 and Eq. 7Eq. 7Eq. 4 are obtained estimated via ordinary least squares (OLS). More complex statistical models such as generalised generalized least squares are not required because the selected catchments do not exhibit a interannual memory longer than a year, as explained in the data section. T(this guarantees the absence of interannual memory guarantees the lack ofstreamflow autocorrelation in annual streamflow, which is a keyan important statistical assumption behind for OLS). Also, ;

a mis en forme : Normal, Sans numérotation ni puces

- when presenting the results, one has to decide of an appropriate statistical significance *p*-value threshold (which is of course a matter of convention). For this paperAdditionally, we chose a p-value threshold of 0.05 for all the discussion of results. In addition, ;

a mis en forme : Normal, Sans numérotation ni puces

- wWe compute elasticity coefficients between anomalies of equal dimensions (in mm/y), and not between relative anomalies (in %) because with the anomalies expressed in mm/y it allows a directthe physically-plausible interpretation range of the valuesis known: [0,1] for $e_{Q/P}$, [-1,0] for e_{Q/E_0} and $e_{Q/A}$ of the coefficients. LastFinally, ;

Eq. 6Eq. 6Eq. 3 and Eq. 7Eq. 7Eq. 4 were solved on a catchment-by-catchment basis, i.e.i.e., we computed 4122 distinct regressions.

We show below (Figure 3Figure 2) an illustration of illustrates this catchment-based computation onusing the example of the Meurthe River @at Raon-l'Étape (727 km²). For: on this catchment, we see that annual streamflow anomalies haveexhibit a well-defined dependency toon both precipitation and synchronicity anomalies, with the dependency toon potential evaporation anomaly being very weak.

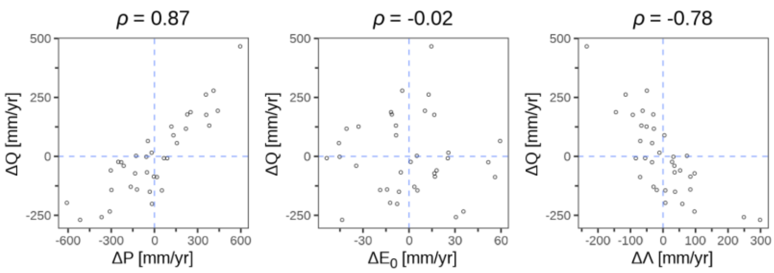

Figure 3. Example of an elasticity plot for the Meurthe River @at Raon-l'Étape (A615103001): each point corresponds to one hydrological year (for this catchment, 36 hydrological years were available, from 1975 to 2021). The Pearson correlations of ΔQ with ΔP, ΔE_0 and $\Delta \Lambda$ are respectively 0.87, -0.02 and -0.78

The visual impression of Figure 3 is confirmed by the results of the linear regressions of Eq. 6Eq. 6 and Eq. 7Eq. 7 in(see Table 3). with vValues of the Student's t-test indicateing that precipitation has a very significantdominant contribution, while the contribution of potential evaporation is not statistically significant. The introduction of the synchronicity increases the R² (from 0.75 to 0.80).

Table 3. Climate elasticity coefficients computed with and without the inclusion of the synchronicity variable Λ for the example catchment (La Meurthe @at Raon-l'Étape)

Formulation	$e_{Q/P}$ [-]	*p-value for $e_{Q/P}$*	e_{Q/E_0} [-]	*p-value for e_{Q/E_0}*	$e_{Q/\Lambda}$ [-]	*p-value for $e_{Q/\Lambda}$*	R^2
$\Delta Q = f(\Delta P, \Delta E_0)$	0.52	*< 0.001*	0.00	*0.99*	–	–	0.75
$\Delta Q = f(\Delta P, \Delta E_0, \Delta \Lambda)$	0.38	*< 0.001*	-0.25	*0.59*	-0.56	*< 0.01*	0.80

a mis en forme : Normal, Sans numérotation ni puces

64 Results

6.14.1 Graphical analysis of anomalies by country

To give provide a general picture overview of the correlation between streamflow anomalies and climatic anomalies, Figure 4 and Figure 5Figure 3Figure 2 presents an aggregated plot for each of the country and for each main climate classdatasets, where we combineing the anomalies of all catchments. At this scale, only general trends are apparent.:

- ~~a~~As expected, streamflow anomaly is clearly positively correlated with precipitation anomaly in all countries;

a mis en forme : Normal, Sans numérotation ni puces

- streamflow anomaly is, overall, very weakly negatively correlated with potential evaporation anomaly, Denmark being the only outlier ~~where~~ with a weak positive correlation ~~is identified~~ (it is mainly due to the year 1990, which was ~~in Denmark~~ a very dry year in Denmark, but with an unusual cold summer). S~~;~~
- ~~s~~treamflow anomaly is clearly negatively correlated to the synchronicity index anomaly (Λ) for all countries. ~~The~~ This negative correlation ~~means~~ indicates that years with a lower Λ (i.e., when precipitation and potential evaporation are more out of phase) yield ~~more~~ greater streamflow~~:~~. T~~t~~his ~~seems~~ observation is perfectly hydro-logical, and conforms to ~~the~~ general observations ~~already~~ previously identified by Pardé (1933a). In the case of Australia, where streamflow anomalies are clearly negatively correlated to the synchronicity index anomaly (Λ) on Figure 4, it is interesting to mention the opposite conclusion of Potter et al. (2005) who wrote that “the inclusion of seasonally varying forcing alone was not sufficient to explain variability in the mean annual water balance”. This surprising conclusion may be an artefact of the index chosen by the authors to describe seasonality.~~;~~
- O~~o~~verall, the most~~only~~ surprising fact is that streamflow anomaly appears ~~clearly~~ more strongly correlated ~~to~~ with the synchronicity index anomaly than ~~to~~ with the potential evaporation anomaly.

	~~ΔQ vs ΔP~~	~~ΔQ vs ΔE₀~~	~~ΔQ vs ΔΛ~~
~~Australia~~			

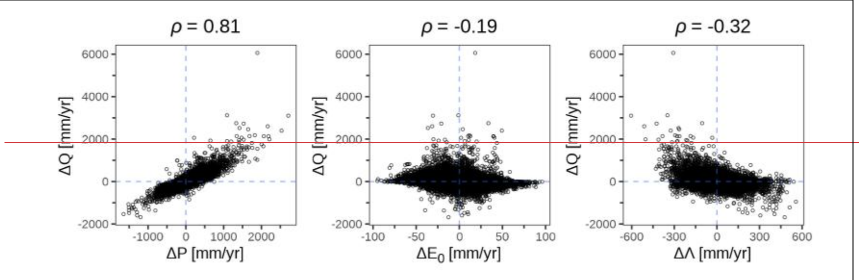

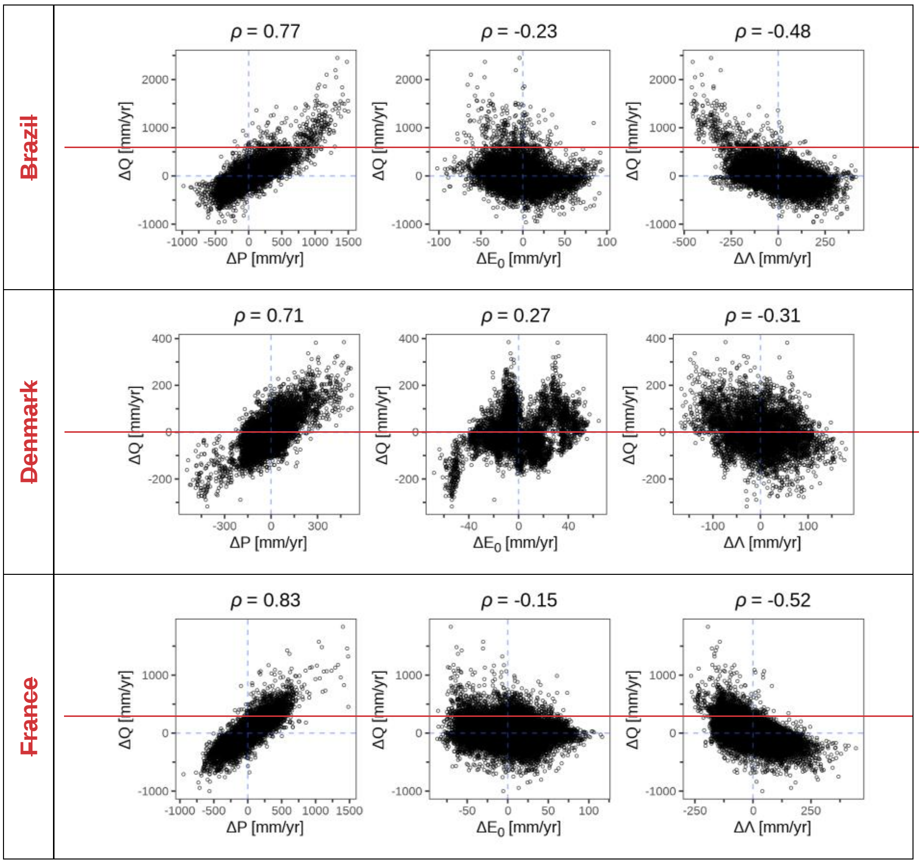
Brazil
Denmark
France
ρ = 0.77
ρ = -0.23
ρ = -0.48
ρ = 0.71
ρ = 0.27
ρ = -0.31
ρ = 0.83
ρ = -0.15
ρ = -0.52
ΔQ [mm/yr]
ΔP [mm/yr]
ΔE0 [mm/yr]
ΔΛ [mm/yr]

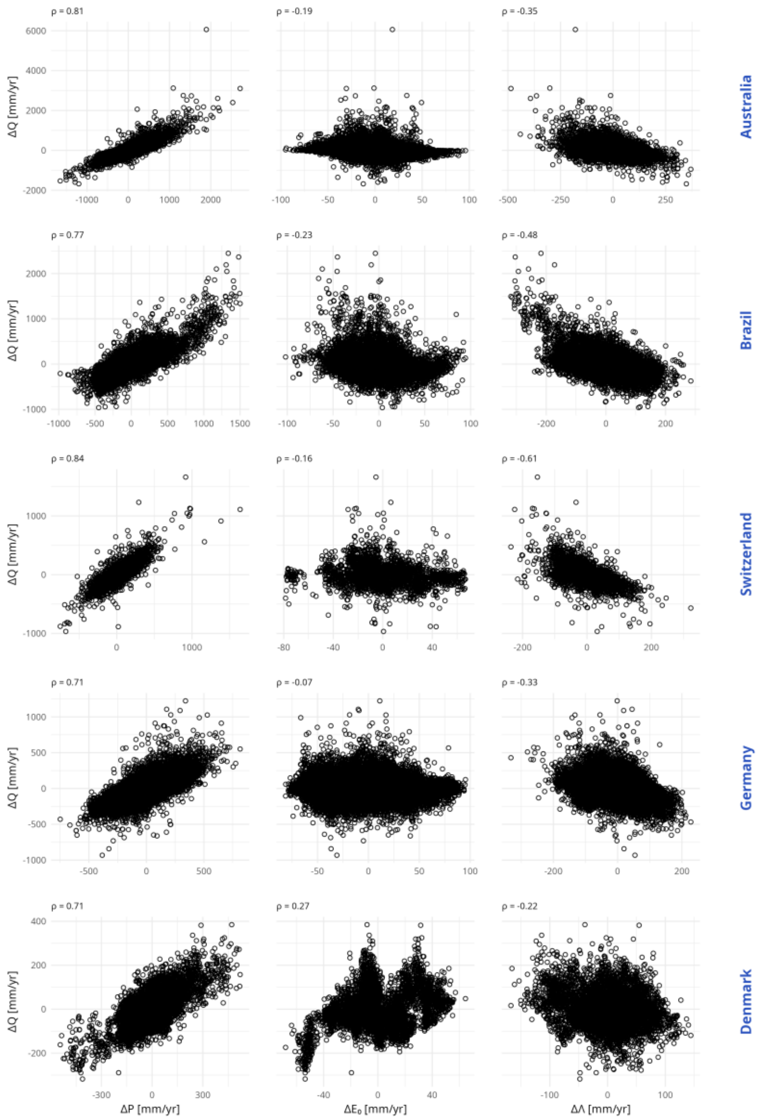

Figure 4 Scatter plots, for each country, between streamflow anomalies ΔQ, and: precipitation anomalies ΔP (left), potential evaporation anomalies ΔE_0 (middle) and synchronicity index anomalies $\Delta \Lambda$ (right). Each point represents one station-year. Above each scatter plot, we provide the corresponding Pearson correlation

a mis en forme : Paragraphes solidaires

a mis en forme : Légende

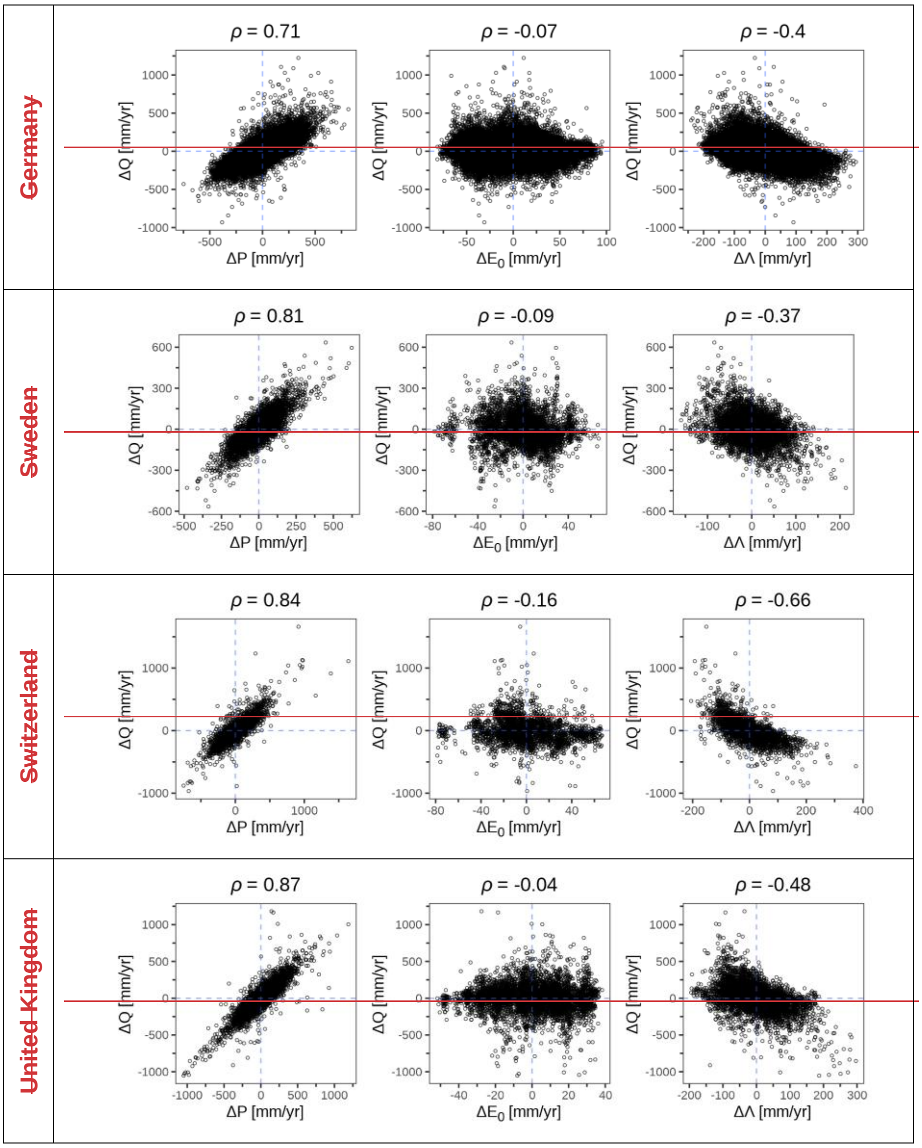
Germany
ρ = 0.71
ρ = -0.07
ρ = -0.4
Sweden
ρ = 0.81
ρ = -0.09
ρ = -0.37
Switzerland
ρ = 0.84
ρ = -0.16
ρ = -0.66
United Kingdom
ρ = 0.87
ρ = -0.04
ρ = -0.48
ΔQ [mm/yr]
ΔP [mm/yr]
ΔE0 [mm/yr]
ΔΛ [mm/yr]

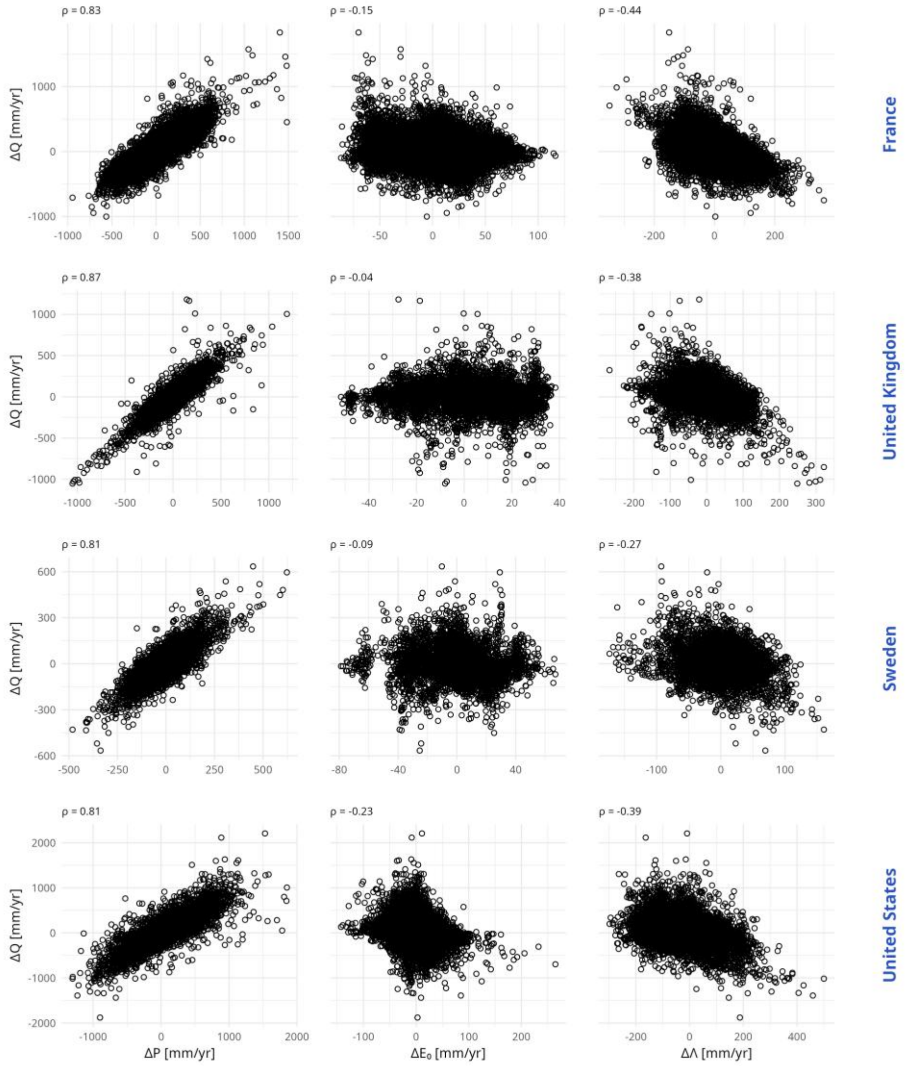

Figure 4. (continuation)

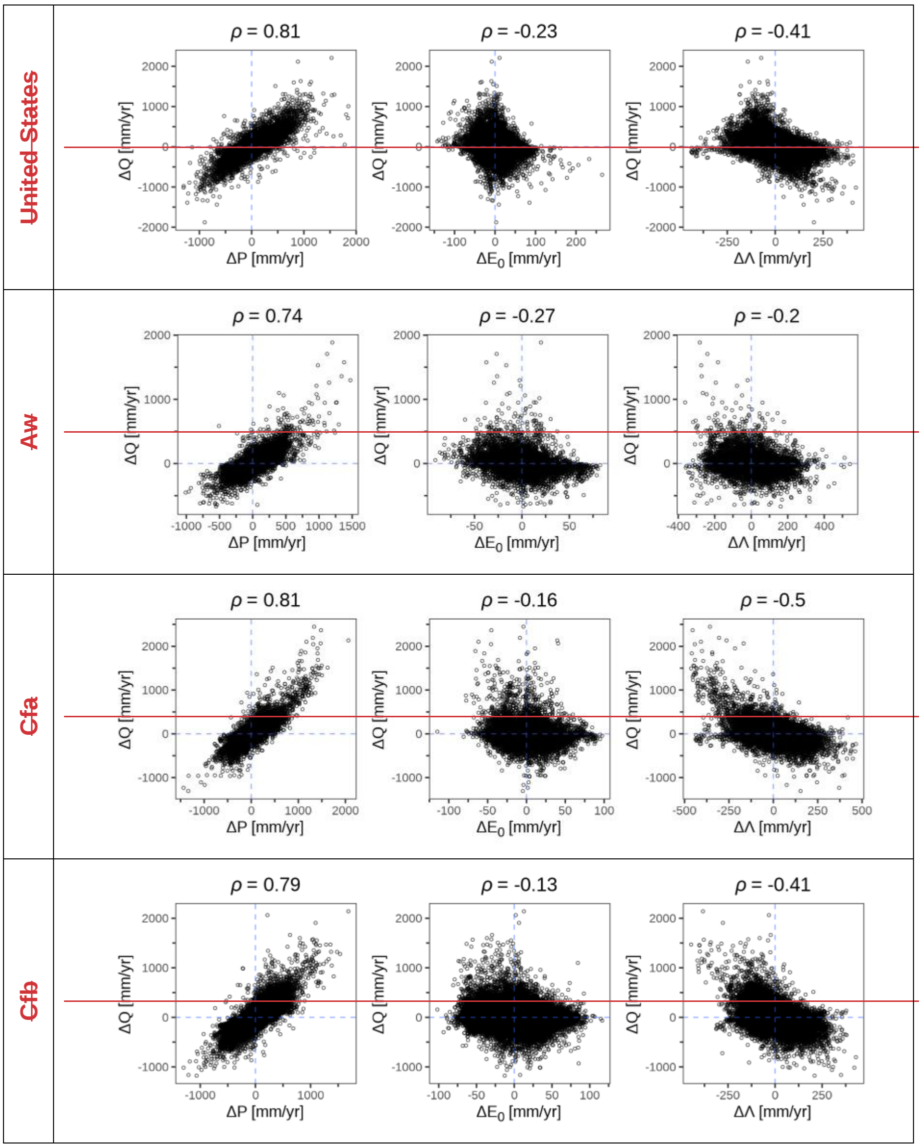
United States
ρ = 0.81
ρ = -0.23
ρ = -0.41
Aw
ρ = 0.74
ρ = -0.27
ρ = -0.2
Cfa
ρ = 0.81
ρ = -0.16
ρ = -0.5
Cfb
ρ = 0.79
ρ = -0.13
ρ = -0.41
ΔQ [mm/yr]
ΔP [mm/yr]
ΔE0 [mm/yr]
ΔΛ [mm/yr]

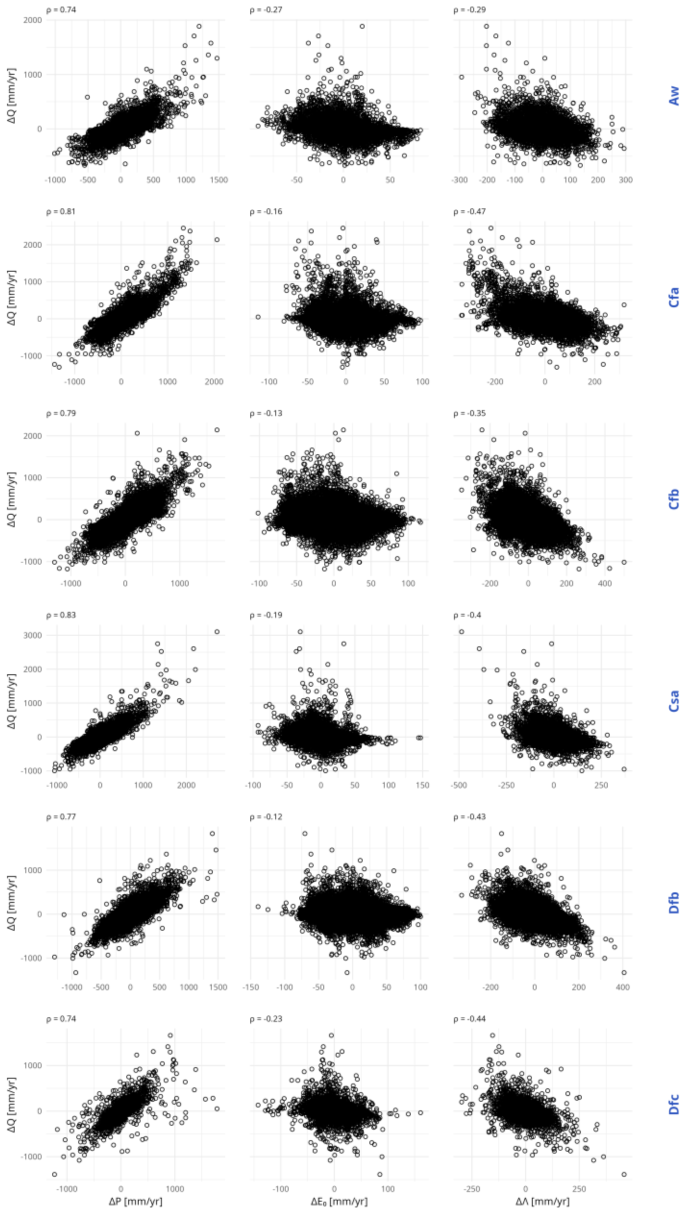

a mis en forme : Centré

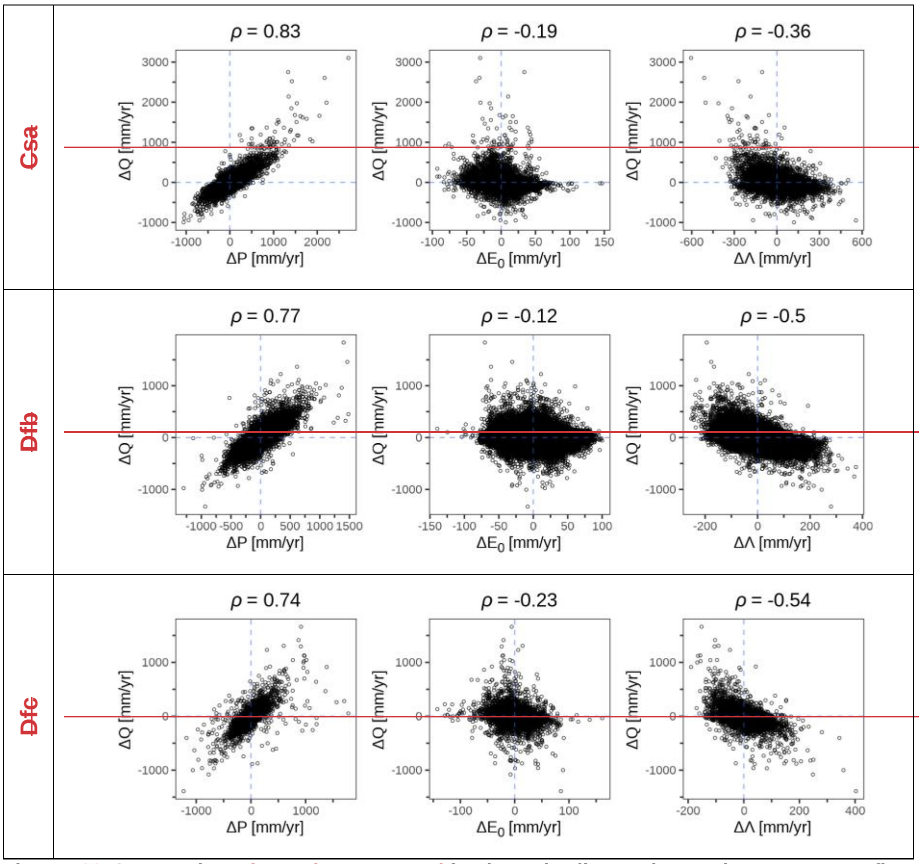

Figure 532. Scatter plots, for each country and for the main climate classes, between streamflow anomalies ΔQ, and: precipitation anomalies ΔP (left), potential evaporation anomalies ΔE_0 (middle) and synchronicity index anomalies $\Delta \Lambda$ (right). Each point represents one station-year. Above the grapheach scatter plot, we have computedprovide the corresponding Pearson correlation

6.2 An example at catchment scale: the Meurthe River @ Raon-l'Étape

We now show one example chosen in France, the Meurthe River (727 km²): on this catchment, with Köppen climate Cfb, annual streamflow anomalies show (Figure 3) a well-defined dependency to both precipitation and synchronicity anomalies, the dependency to potential evaporation anomaly being very weak.

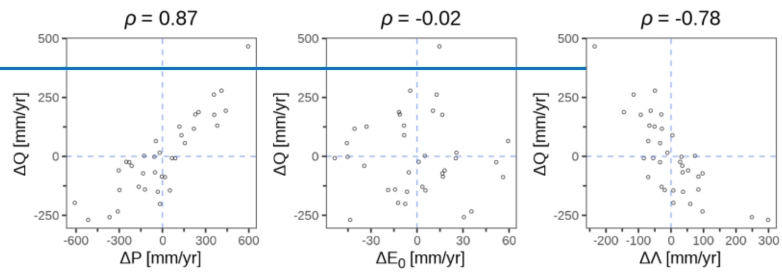

~~**Figure 3. Example of an elasticity plot for the Meurthe River @ Raon-l'Étape (A615103001): each point corresponds to one hydrological year (for this catchment, 36 hydrological years were available, from 1975 to 2021). The Pearson correlations of ΔQ with ΔP, ΔE_0 and $\Delta \Lambda$ are respectively 0.87, -0.02 and -0.78**~~

~~The visual impression is confirmed by the results of the linear regressions of Eq. 3 and Eq. 4 (Table 3), with values of the Student t-test indicating that precipitation has a very significant contribution, while the contribution of potential evaporation is not significant. The introduction of the synchronicity increases the R² (from 0.75 to 0.80) but the potential evaporation elasticity estimate remains not significant.~~

~~**Table 3. Climate elasticity coefficients computed with and without the inclusion of the synchronicity variable Λ for the example catchment (La Meurthe @ Raon-l'Étape)**~~

Formulation	$e_{Q/P}$ [-]	*p-value for $e_{Q/P}$*	e_{Q/E_0} [-]	*p-value for e_{Q/E_0}*	$e_{Q/\Lambda}$ [-]	*p-value for $e_{Q/\Lambda}$*	R²
$\Delta Q = f(\Delta P, \Delta E_0)$	0.52	*< 0.001*	0.00	*0.99*	–	–	0.75
$\Delta Q = f(\Delta P, \Delta E_0, \Delta \Lambda)$	0.38	*< 0.001*	-0.25	*0.59*	-0.56	*< 0.01*	0.80

~~6.3~~84.2 Overall results by catchment

We now ~~analyse~~analyze the results obtained for each of the 4122 catchments. Table 4~~Table 4Table 4~~ shows the statistics of the individual regressions~~,~~ for the classical case ~~(i.e.,~~ when ~~no~~ synchronicity is not included ~~in the regression~~as a predictor~~)~~. This analysis reveals that~~used (the classical case). It shows that~~ for all ~~the~~ countries and all ~~the~~ climate groups, ~~:~~

~~the value of~~ the precipitation elasticity of streamflow is almost always significant at the 0.05 level. On the other hand, ~~;~~

a mis en forme : Normal, Sans numérotation ni puces

- the value of the potential evaporation elasticity of streamflow is not frequently significant at the 0.05 level. In addition, the;
- regression allows identifyingidentifies values of physically realistic precipitation elasticity values (between 0 and 1) which are almost always (i.e.for almost all catchments (for 93% of the catchments worldwide, and a minimum at the minimum forof 80% of the cases foracross the different groupings), physically-realistic, i.e. comprised between 0 and 1 whereas potential evapotranspiration elasticity is frequently physically unrealistic with only 6% of values in the range [0, 1] globally..

Table 4. Linear regression results by country for Eq. 6Eq. 6Eq. 3 when regression uses two independent variables *P* and *E₀* to explain streamflow anomaly

Region or climate class	Total number of catchments	Percentage of catchments where $e_{Q/P}$ was		Percentage of catchments where e_{Q/E_0} was		Mean adjusted R²
		significant at the 0.05 level	*significant and in the range [0,1]*	significant at the 0.05 level	*significant and* in the range [-1,0]	
By country						
Australia	546	100%	97%	18%	9%	0.6867
Brazil	636	95%	86%	12%	4%	0.6461
Denmark	202	100%	100%	9%	0%	0.5551
France	628	100%	93%	21%	7%	0.7371
Germany	1094	94%	93%	18%	9%	0.5047
Sweden	152	100%	87%	20%	7%	0.6865
Switzerland.	73	100%	86%	8%	0%	0.7775
UK	136	99%	89%	25%	2%	0.7675
USA	655	99%	95%	9%	4%	0.6765
By climate class						
Aw	344	93%	91%	16%	7%	0.6260
Cfa	364	100%	90%	3%	0%	0.6966
Cfb	1746	98%	94%	18%	7%	0.6360
Csa	196	99%	96%	7%	1%	0.6967
Dfb	956	96%	94%	21%	9%	0.5856
Dfc	132	99%	80%	29%	10%	0.7371
World	**4122**	**97%**	**93%**	**16%**	**6%**	**0.6361**

Aw - Tropical savanna climate with dry winter, Cfa – Temperate climate without dry season with hot summer, Cfb – Temperate climate without dry season with warm summer, Csa – Temperate climate with dry and hot summers, Dfb – Continental climate without dry season with warm summer, Dfc – Continental climate without dry season with cold summer

Table 5Table 5Table 5 shows presents the same statistics, when the anomaly of synchronicity anomaly ($\Delta\Lambda_n$) is introduced into the elasticity equation regression (Eq. 7). It This analysis shows that :

- the average efficiency of the regression equation rises visibly increases foacrossr all the countries and all the climate groups (see also Figure 6Figure 4Figure

a mis en forme : Police :10 pt, Gras

a mis en forme : Police :10 pt, Gras

a mis en forme : Police :10 pt, Gras

a mis en forme : Police :10 pt, Gras

a mis en forme : Police :10 pt, Gras

a mis en forme : Police :10 pt, Gras

a mis en forme : Normal, Sans numérotation ni puces, Autoriser lignes veuves et orphelines

4). NaturallyWhile, an increase is expected when one adds an independent additional variable predictor is added toin a regression, please note that we are presenting adjusted R^2 values, which are designed to take that issue into account. T-he average additional explained variance lies in the range but depending on the groups, the average additional explained variance varies between 3 % %-and 10 % (7 6 % globally), depending on the group, which and we consider it as significant noticeable improvement. Additionally, ;

for 64 % of the catchments, the anomaly of synchronicity anomaly ($\Delta\Lambda_n$) provides is a significant contribution to the regression for 64 % of the catchments, (to b,e compared to only 23 % for potential evaporation).;

- AlsoMore important,
- introducing the anomaly ofthe introduction of the synchronicity anomaly ($\Delta\Lambda_n$) does not modify the significance of the two other two elasticity coefficients $e_{Q/P}$ and e_{Q/E_0}: . A slight increasewe even have a slight increase is observed in the of the proportion of catchments where e_{Q/E_0} coefficient is significant at the 0.05 level (from 16 % to 23 %).;
- Moreover, the utilization introducing the anomaly of synchronicityof $\Delta\Lambda_n$ does not degrade the physical realism of the elasticity coefficients $e_{Q/P}$ and e_{Q/E_0}: we even hav. Once again, ae a slight increase is observed inof the proportion of catchments where $e_{Q/P}$ coefficient is significant and in the physical range [0,1] (from 93 % to 94 %), and where $e_{Q/P}$ coefficient is significant and in the physical range [0,1] (from 93 % to 94 %) and where e_{Q/E_0} coefficient is significant at the 0.05 level and in the physical range [-1,0] (from 6 % to 11 %). ;

Finally, there are only two countries (Switzerland and Brazil) and one climate type (*Dfc* – Continental climate without dry season with cold summer) which differ from the others by theshowed lower relevance of the synchronicity index compared to other regions. We attribute this reduced relevance in Switzerland and climate zone *Dfc* to the Our interpretation of this lesser relevance is as follows: for Switzerland and climate zone Dfc we attribute it to the essentially energy-limited nature of the catchments as our selection criteria for Switzerland prioritized high-elevation catchments with minimal anthropogenic impact (see also the Discussion section and Figure 9). Last, note that in all groupings except Dfc, the number of catchments where $e_{Q/\Lambda}$ is significant at the

a mis en forme : Normal, Sans numérotation ni puces, Autoriser lignes veuves et orphelines

0.05 level exceeds that where the e_{Q/E_0} coefficient is significant at the same level.y limited nature of the catchments

(because we wanted catchments with minimal anthropogenic impact, we have selected in Switzerland essentially catchments at high elevations). Note however that in all groupings except Dfc, there are more catchments where $e_{Q/A}$ is significant at the 0.05 level than catchments where e_{Q/E_0} coefficient is significant at the same level.

a mis en forme : Normal, Sans numérotation ni puces, Autoriser lignes veuves et orphelines

Table 5. Linear regression results by country for Eq. 7Eq. 7Eq. 4 when regression uses three independent variables to explain streamflow anomaly (to allow for comparison, the last column reports the mean R^2 of Table 4Table 4Table 4)

Country	Total number of catchments	Percentage of catchments where $e_{Q/P}$ was		Percentage of catchments where e_{Q/E_0} was		Percentage of catchments where $e_{Q/\Lambda}$ was		Mean adj. R^2	*Mean adj. R^2 from Table 4Table 4Table 4*
		significant at the 0.05 level	*significant and in the range [0,1]*	significant at the 0.05 level	*significant and in the range [-1,0]*	significant at the 0.05 level	*significant and in the range [-1,0]*		
By country									
Australia	546	100%	9798%	4138%	2420%	87%	8783%	0.78776	*0.670.68*
Brazil	636	90%	8384%	13%	5%	2625%	2522%	0.6864	*0.610.64*
Denmark	202	98100%	98100%	76%	0%	4344%	4344%	0.606156	*0.510.55*
France	628	99100%	9796%	2730%	1213%	82%	7980%	0.7977	*0.710.73*
Germany	1094	97%	9697%	2627%	16%	79%	7876%	0.6057	*0.470.50*
Sweden	152	100%	910%	2324%	5%	4041%	4038%	0.7269	*0.650.68*
Switzerl.land	73	9096%	7582%	58%	0%	2122%	1921%	0.7876	*0.750.77*
UK	136	99%	90%	4138%	11%	62%	5859%	0.8281	*0.750.76*
USA	655	9899%	96%	11%	45%	57%	52%	0.7371	*0.650.68*
By climate class									
Aw	359344	9190%	9088%	1918%	1110%	4442%	4440%	0.6867	*0.6260*
Cfa	364	9798%	9091%	9%	21%	5251%	5047%	0.7574	*0.6966*
Cfb	1746	99%	96%	2728%	1514%	76%	7574%	0.71	*0.6260*
Csa	197	9899%	9697%	1917%	42%	4643%	4637%	0.7473	*0.6967*
Dfb	956	9798%	96%	2527%	1314%	68%	65%	0.66	*0.5856*
Dfc	132	9698%	8182%	2830%	68%	2730%	2629%	0.76	*0.7371*
World	**4122**	**97%**	**94%**	**23%**	**11%**	**64%**	**6261%**	**0.7067**	***0.6361***

Aw - Tropical savanna climate with dry winter, Cfa – Temperate climate without dry season with hot summer, Cfb – Temperate climate without dry season with warm summer, Csa – Temperate climate with dry and hot summers, Dfb – Continental climate without dry season with warm summer, Dfc – Continental climate without dry season with cold summer

- **a mis en forme :** Police :9 pt, Gras, Italique
- **a mis en forme :** Police :9 pt, Italique
- **a mis en forme :** Police :9 pt, Italique
- **a mis en forme :** Police :9 pt, Italique
- **a mis en forme :** Police :9 pt, Italique
- **a mis en forme :** Police :9 pt, Italique
- **a mis en forme :** Police :9 pt, Italique
- **a mis en forme :** Police :9 pt, Italique
- **a mis en forme :** Police :9 pt, Italique
- **a mis en forme :** Police :9 pt, Italique

75 Discussion

Figure 6Figure 4Figure 4 illustrates the improvement inof explanatory capacity in of the regressions due to the introduction of the synchronicity anomalies. While considerable variability exists, and some catchments show equivalent performance between the two regression models (indicated by points on the 1:1 line), the graph confirms that for many catchments (approximately 66 % of the dataset, where $e_{Q/A}$ was significant at the 0.05 level), accounting for synchronicity anomalies visibly improves the linear regression's efficiencyefficiency of the linear regression. Because the adjusted R^2 shows the same trend as the classical R^2, this is clearly not a simple effect of the increase of independent variables in the regression.There is of course a lot of variability, as well as catchments for which the two regression models are equivalent (points on the 1:1 line) but overall the graph confirms visually that for many catchments (cf. the two third of the dataset where $e_{Q/A}$ was significant at the 0.05 level), accounting for synchronicity anomalies brings a visible improvement in the efficiency of the linear regression.

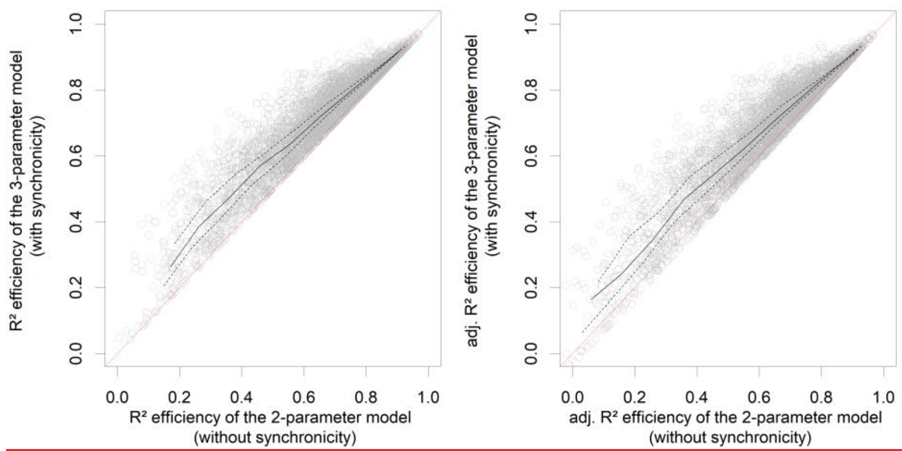

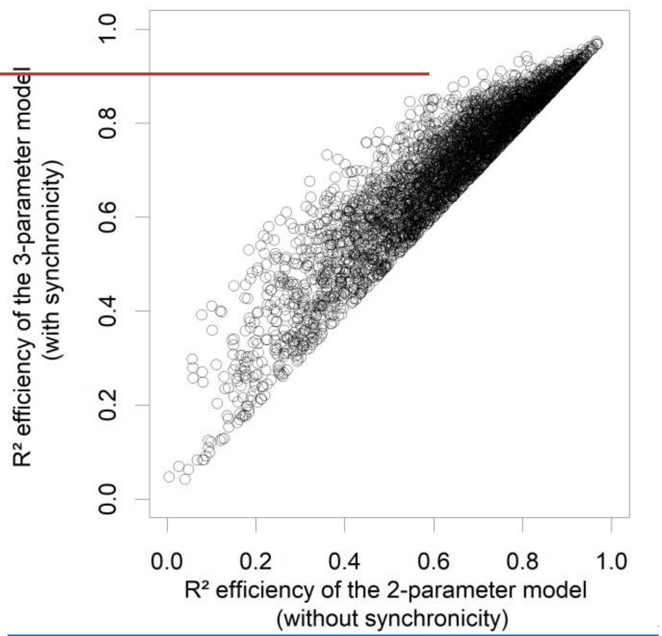

Figure 64. Comparison of the performances of the 2-parameter streamflow elasticity model (Eq. 6Eq. 6Eq. 3, which does not account for *P*-E_0 synchronicity) and the 3-parameter model (Eq. 7Eq. 7Eq. 4, which does). Each point represents one of the 4122 catchments of our dataset. The solid line represents the median, and the dashed lines represent the first and the third quartiles. As measure of efficiency, we use the R² on the left plot and the adjusted R² on the right one

a mis en forme : Centré

In Figure 7, we summarize the significativity of the $e_{Q/\Lambda}$ coefficient across all the Köppen climate classes represented in our dataset: $e_{Q/\Lambda}$ is significative at the 0.05 level for 50 % of the catchments in 11 classes (representing 79% of the catchments).

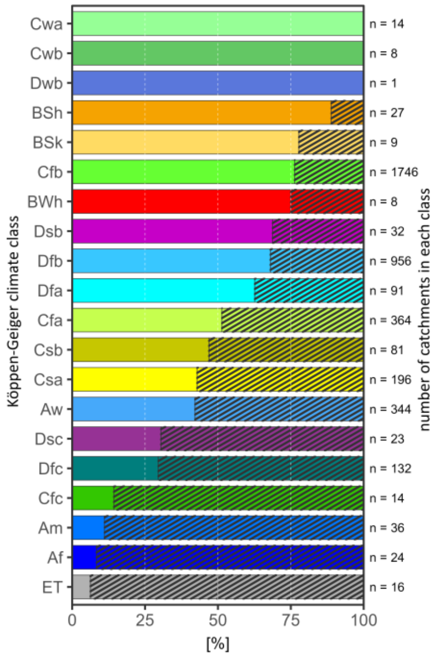

Figure 7. significativity of the P-E$_0$ synchronicity anomalies by Köppen climate class: the dashed area represents the proportion of catchments for which synchronicity was not deemed significant

Also, Figure 8Figure 5 shows the geographic distribution of the catchments where the P-E$_0$ synchronicity had a significant contribution to explain streamflow anomalies (with a p-value threshold of 0.05). The map brings some further elements to Table 5Table 5Table 5 and illustrate that there are sub-regions where the coefficient $\boldsymbol{e_{Q/\Lambda}}$ is mostly not significant at the 0.05 level. Based on our knowledge of the climatic specificities of each country, this seems to be possibly correlated to higher rainfall (cf. the Danish dataset, with the particular behavior of the West of Jutland, the case of Florida in the US, the case of the Scottish catchments in Great Britain) and/or to colder areas (cf. the Swiss, Swedish and US datasets).

Code de champ modifié

a mis en forme : Police :Non Gras

a mis en forme : Indice

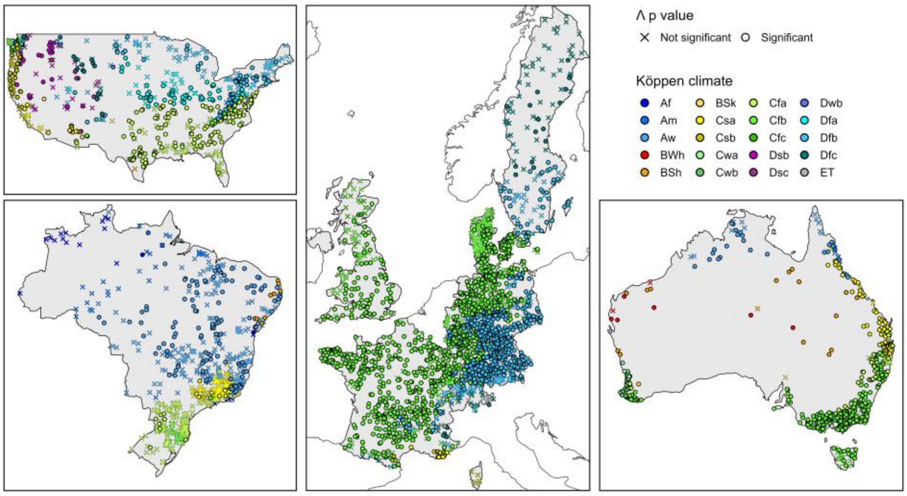

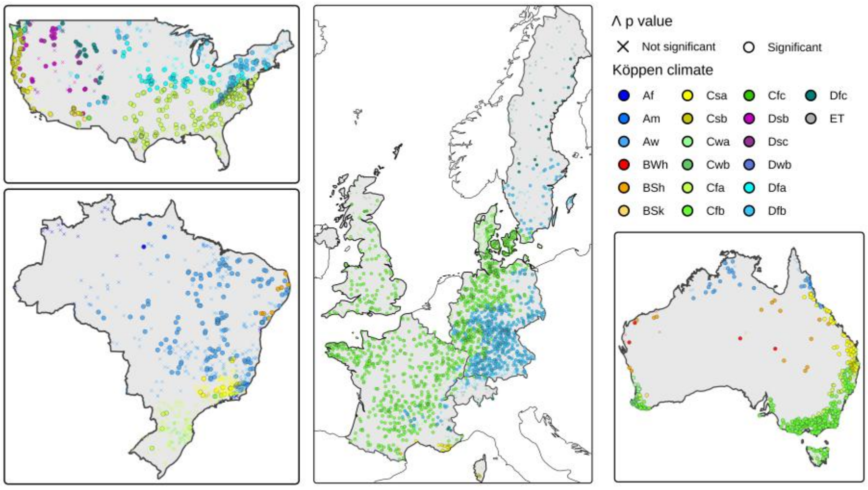

Figure 85. map of the 4122 catchments used in this study, each catchment is represented by either a circle (where the P-E_0 synchronicity anomalies had a significant contribution to explain streamflow anomalies) or a cross (where it was not significant at the 0.05 level). The color of circles and crosses corresponds to the Köppen climate classes

a mis en forme : Légende

To verify this hypothesis, ~~we have plotted in~~ Figure 9~~Figure 6~~ presents the p-values of the 4122 $e_{Q/\Lambda}$ coefficients as a function of the humidity index P/E$_0$. T~~: t~~his graph clearly indicates that most of the humid catchments (Humidity index > 2) lack sensitivity to the P-E$_0$ seasonality, and this pattern is ~~probably~~ likely the main explanation ~~of~~ for the geographical patterns observed~~visible~~ in Figure 8~~Figure 5~~.

a mis en forme : Centré

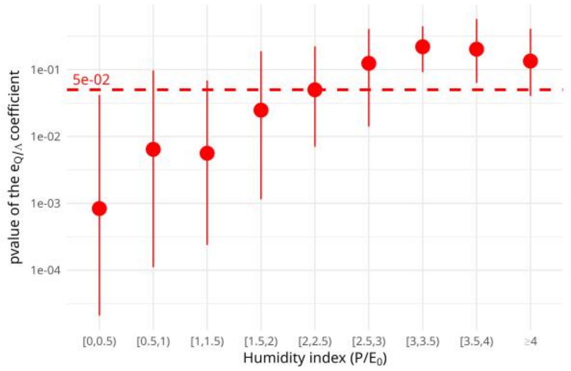

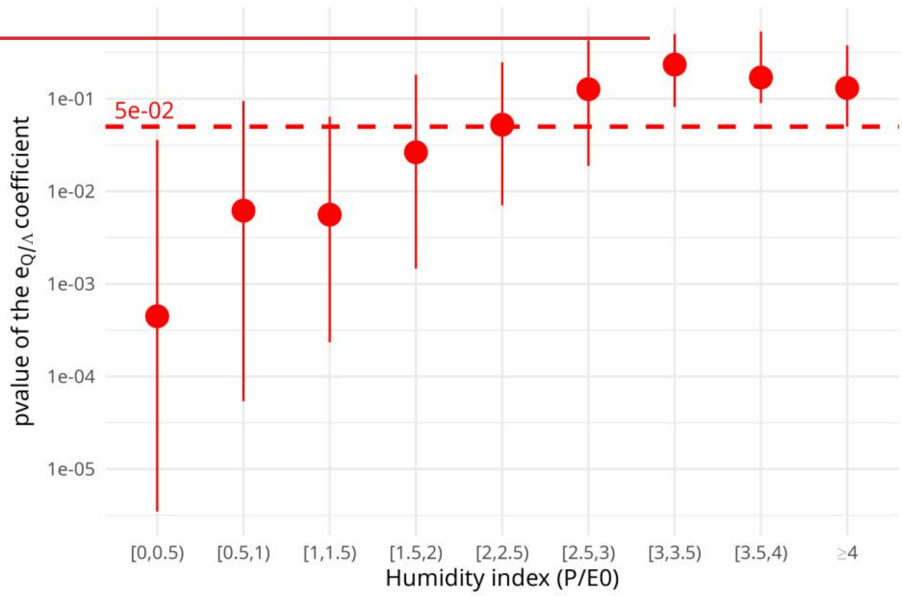

Figure 9~~6~~: distribution of the p-~~va~~values of the 4122 $e_{Q/\Lambda}$ coefficients as a function of the humidity index P/E0. The red points represent the median, the bar represent the interquartile range, and the dashed line represents the 0.05 threshold.

~~8~~6 Conclusion

~~8.1~~6.1 Synthesis

In this paper, we investigated the dependency between streamflow elasticity and the synchronicity of precipitation and potential evaporation, using a dataset of 4122 catchments located in Europe, Australia, North America and South America. Our analysis provided three main findings. First, we empirically verified the strong correlation among streamflow anomalies, annual precipitation anomalies, and synchronous *P*-E_0 anomalies. Second, we demonstrated that the role of the synchronicity between *P* and E_0 in explaining streamflow anomalies is significantly more important than that of E_0 anomalies. Finally, we showed that introducing synchronicity between precipitation and potential evaporation as an ~~independent~~additional predictor ~~variable~~ in the linear regression clearly improves the prediction of annual streamflow variability.

~~In this paper, we investigated the dependency between streamflow elasticity and the synchronicity of precipitation and potential evaporation, using a dataset of 4122 catchments located in Europe, Australia, North America and South America.~~

- ~~we verified empirically the good correlation existing between streamflow anomalies, the anomalies of annual precipitation, and the anomalies of synchronous *P*-E_0 amounts;~~
- ~~we demonstrated that the role of the synchronicity between *P* and E_0 is far more important to explain streamflow anomalies than the role of the anomalies of E_0;~~
- ~~we showed that introducing the synchronicity between precipitation and potential evaporation as an independent variable in the linear regression clearly improves the prediction of annual streamflow variability.~~

~~8.6~~6.2 Perspectives

Notwithstanding these positive results, some estimated elasticity values remain outside of their physically acceptable domain (i.e., [0,1] for $e_{Q/P}$ and [-1,0] for e_{Q/E_0} and $e_{Q/\Lambda}$). For precipitation elasticity ($e_{Q/P}$), 93% of the catchments were within the physical range, out of a total of 97% where precipitation elasticity was significant. For potential evaporation elasticity (e_{Q/E_0}), a lack of physical realism occurs in most of the cases (i.e., only 11% of the catchments were within the physical range, out of a total of 23% where potential evaporation elasticity was significant). This is very likely due to a sensitivity problem in the regression, which contributes to the difficulty in obtaining realistic elasticity coefficients. Finally, for synchronicity elasticity ($e_{Q/\Lambda}$), 61% of the catchments were within the physical range out of a total of 64% where synchronicity elasticity was significant. In the future, we aim to investigate alternative statistical models that could better constrain the elasticity coefficients within their physically realistic domain.

~~Notwithstanding with the above positive results, some estimated elasticity values remain outside of their physically acceptable domain (i.e. [0,1] for $e_{Q/P}$ and [-1,0] for e_{Q/E_0} and $e_{Q/A}$). For precipitation elasticity $e_{Q/P}$, we had 94~~93~~% of the catchments in the physical range for a total of 97% of the catchments where precipitation elasticity was significant. For potential evaporation elasticity e_{Q/E_0}, lack of physical realism occurs in most of the cases (i.e. we had only 11% of the catchments in the physical range for a total of 23% of the catchments where potential evaporation elasticity was significant), very likely a problem of sensitivity in the regression, which causes this difficulty in obtaining realistic elasticity coefficients. Last for synchronicity elasticity $e_{Q/A}$, we had 62~~1~~% of the catchments in the physical range for a total of 64% of the catchments where synchronicity elasticity was significant. In the future, we wish to investigate more alternative statistical models that could better constrain the identification of the elasticity coefficients within their physically realistic domain.~~

~~10~~7 Acknowledgements

The authors would like to acknowledge the many individuals that worked to make available the hydrological datasets used in this paper. Special thanks are due to the two anonymous reviewers, to the Editor as well as to Charles Perrin and Guillaume Thirel for their reviews and suggestions and to Laurent Strohmenger for his help with the Köppen-Geiger classification.

~~11~~8 Funding

This research has been funded in part by the Agence Nationale de la Recherche (projects CIPRHES ANR-20-CE04-0009 and DRHYM ANR-22-CE56-0007).

~~12~~9 Author contributions

VA: conceptualization and writing, GMG: computations, figures, discussion, writing (review and editing), AL: computations, discussion, figures, JL: discussion, writing (review and editing)

~~13~~10 Competing interests

The authors declare that they have no conflict of interest.

~~14~~11 References

Addor, N., A. J. Newman, N. Mizukami, and M. P. Clark. 2017. The CAMELS data set: catchment attributes and meteorology for large-sample studies. Hydrol. Earth Syst. Sci., 21: 5293-5313. https://dx.doi.org/10.5194/hess-21-5293-2017

Almagro, A., Oliveira, P.T.S., Alves Meira Neta, A., Roy, T., Troch, P. 2021. CABra: a novel large-sample dataset for Brazilian catchments. Hydrol. Earth Syst. Sci., 25: 3105–3135. https://doi.org/10.5194/hess-25-3105-2021

Andréassian, V., L. Coron, J. Lerat, and N. Le Moine. 2016. Climate elasticity of streamflow revisited – an elasticity index based on long-term hydrometeorological records. Hydrol. Earth Syst. Sci., 20: 4503–4524, https://dx.doi.org/10.5194/hess-20-4503-2016

Berghuijs, W.R., Sivapalan, M., Woods, R.A., & Savenije, H.H. 2014. Patterns of similarity of seasonal water balances: A window into streamflow variability over a range of time scales. Water Resources Research, 50, 5638-5661. https://doi.org/10.1002/2014WR015692

Chiew, F.H.S. 2006. Estimation of rainfall elasticity of streamflow in Australia. Hydrological Sciences Journal, 51: 613–625. https://doi.org/10.1623/hysj.51.4.613

Coutagne, A. and E. de Martonne. 1934. De l'eau qui tombe à l'eau qui coule – évaporation et déficit d'écoulement. IAHS, vol 97-128.

Coxon, G., N. Addor, J. P. Bloomfield, J. Freer, M. Fry, J. Hannaford, N. J. K. Howden, R. Lane, M. Lewis, E. L. Robinson, T. Wagener, and R. Woods. 2020. CAMELS-GB: hydrometeorological time series and landscape attributes for 671

Code de champ modifié

catchments in Great Britain. Earth Syst. Sci. Data, 12: 2459-83. https://dx.doi.org/10.5194/essd-12-2459-2020

de Lavenne, A., V. Andréassian, L. Crochemore, G. Lindström, & B. Arheimer. 2022. Quantifying pluriannual hydrological memory with Catchment Forgetting Curves. Hydrol. Earth Syst. Sci., 26: 2715–2732, https://doi.org/10.5194/hess-26-2715-2022

de Lavenne, A. & V. Andréassian. 2018. Impact of climate seasonality on catchment yield: a parameterization for commonly-used water balance formulas. J. Hydrol., 558: 266–274. https://dx.doi.org/10.1016/j.jhydrol.2018.01.009

Delaigue, O., Mendoza Guimarães, G., Brigode, P., Génot, B., Perrin, C., Soubeyroux, J.M., Janet, B. Addor, N. & Andréassian, V. 2024. CAMELS-FR dataset: A large-sample hydroclimatic dataset for France to explore hydrological diversity and support model benchmarking. Earth Syst. Sci. Data Discuss. [preprint]. https://doi.org/10.5194/essd-2024-415

Donohue, R., Roderick, M.L., McVicar, T.R. 2012. Roots, storms and soil pores: incorporating key ecohydrological processes into Budyko's hydrological model. J. Hydrol., 436-437: 35-50. https://doi.org/10.1016/j.jhydrol.2012.02.033

Dooge, J.C.I., 1992. Sensitivity of runoff to climate change: A Hortonian approach. Bulletin of the American Meteorological Society, 73: 2013-2024. https://doi.org/10.1175/1520-0477(1992)073<2013:SORTCC>2.0.CO;2

Feng, X., Vico, G., Porporato, A., 2012. On the effects of seasonality on soil water balance and plant growth. Water Resour. Res., 48. https://doi.org/10.1029/2011WR011263

Feng, X. Thompson, S.E., Woods, R., & Porporato, I. 2019. Quantifying asynchronicity of precipitation and potential evapotranspiration in Mediterranean climates. Geophysical Research Letters. https://doi.org/10.1029/2019GL085653

Fowler, K. J. A., Zhang, Z., and Hou, X.: CAMELS-AUS v2: updated hydrometeorological time series and landscape attributes for an enlarged set of catchments in Australia, Earth Syst. Sci. Data Discuss. [preprint], https://doi.org/10.5194/essd-2024-263, in review, 2024.

Hickel, K., Zhang, L., 2006. Estimating the impact of rainfall seasonality on mean annual water balance using a top-down approach. J. Hydrol. 331: 409–424. https://doi.org/10.1016/j.jhydrol.2006.05.028

a mis en forme : Anglais (États-Unis)

a mis en forme : Anglais (États-Unis)

a mis en forme : Anglais (États-Unis)

Code de champ modifié

a mis en forme : Anglais (États-Unis)

a mis en forme : Anglais (États-Unis)

Höge, M., Kauzlaric, M., Siber, R., Schönenberger, U., Horton, P., Schwanbeck, J. and Floriancic, M. G. and Viviroli, D. and Wilhelm, S. and Sikorska-Senoner, A.E., Addor, N., Brunner, M., Pool, S., Zappa, M. and Fenicia, F., 2023. CAMELS-CH: hydro-meteorological time series and landscape attributes for 331 catchments in hydrologic Switzerland. Earth Syst. Sci. Data, 15: 5755-5784. https://doi.org/10.5194/essd-15-5755-2023

Jawitz, J.W., Klammler, H. and Reaver, N.G.F. 2022. Climatic asynchrony and hydrologic inefficiency explain the global pattern of water availability. Geophysical Research Letters, 49, e2022GL101214. https://doi.org/10.1029/2022GL101214

Koster, R.D., and M.J. Suarez. 1999. A simple framework for examining the interannual variability of land surface moisture fluxes. Journal of Climate, 12: 1911-1917. https://doi.org/10.1175/1520-0442(1999)012<1911:ASFFET>2.0.CO;2

Leopold, L.B. 1974. Water: A Primer. WH Freeman & Co, 172 p.

Loritz, R., Dolich, A., Acuña Espinoza, E., Ebeling, P., Guse, B., Götte, J., Hassler, S. K., Hauffe, C., Heidbüchel, I., Kiesel, J., Mälicke, M., Müller-Thomy, H., Stölzle, M., and Tarasova, L. 2024. CAMELS-DE: hydro-meteorological time series and attributes for 1555 catchments in Germany, Earth Syst. Sci. Data Discuss. [preprint], https://doi.org/10.5194/essd-2024-318

Liu, J., Koch, J., Stisen, S., Troldborg, L., Højberg, A. L., Thodsen, H., Hansen, M. F. T., and Schneider, R. J. M. 2024. CAMELS-DK: Hydrometeorological Time Series and Landscape Attributes for 3330 Catchments in Denmark, Earth Syst. Sci. Data Discuss. [preprint], https://doi.org/10.5194/essd-2024-292

Milly, P.C.D. 1994. Climate, interseasonal storage of soil water, and the annual water balance. Advances in Water Resources, 17(1–2), 19–24. https://doi.org/10.1016/0309-1708(94)90020-5

Muelchi, R., Rössler, O., Schwanbeck, J., Weingartner, R., Martius, O. 2022. An ensemble of daily simulated runoff data (1981–2099) under climate change conditions for 93 catchments in Switzerland (Hydro-CH2018-Runoff ensemble). Geosci Data J., 9: 46–57. https://doi.org/10.1002/gdj3.117

Oudin, L., Hervieu, F., Michel, C., Perrin, C., Andréassian, V., Anctil, F. & Loumagne, C. 2005. Which potential evapotranspiration input for a rainfall-runoff model? Part 2 – Towards a simple and efficient PE model for rainfall-runoff modelling. Journal of Hydrology, 303: 290-306, https://dx.doi.org/10.1016/j.jhydrol.2004.08.026

Padrón, R.S., Gudmundsson, L., Greve, P., and Seneviratne, S.I. 2017. Large-scale controls of the surface water balance over land: Insights from a systematic review and meta-analysis. Water Resources Research, 53, 9659-9678. https://doi.org/10.1002/2017WR021215

Pardé, M., 1933a. Fleuves et rivières. Armand Collin, Paris. 224 p.

Pardé, M., 1933b. L'abondance des cours d'eau. Revue de Géographie Alpine, 21 (3): 497–542. https://www.persee.fr/doc/rga_0035-1121_1933_num_21_3_5370

Peel, M.C., Finlayson, B.L., McMahon, T.A. 2007. Updated world map of the Köppen–Geiger climate classification, Hydrol. Earth System Sci., 11(5):1633-1644. https://doi.org/10.5194/hess-11-1633-2007

Potter, N.J., Zhang, L., Milly, P.C.D., McMahon, T.A., Jakeman, A.J., 2005. Effects of rainfall seasonality and soil moisture capacity on mean annual water balance for Australian catchments. Water Resour. Res. 41 (6). https://doi.org/10.1029/2004wr003697

Roderick, M.L., Farquhar, G.D., 2011. A simple framework for relating variations in runoff to variations in climatic conditions and catchment properties. Water Resour. Res., 47. https://doi.org/10.1029/2010WR009826

Sankarasubramanian, A., Vogel, R.M., Limbrunner, J.F., 2001. Climate elasticity of streamflow in the United States. Water Resour. Res., 37(6): 1771-1781. https://doi.org/10.1029/2000wr900330

Schaake, J., Liu, C., 1989. Development and application of simple water balance models to understand the relationship between climate and water resources, New Directions for Surface Water Modeling. IAHS Red Book series n°181, Wallingford, pp. 343-352. https://iahs.info/uploads/dms/7849.343-352-181-Schaake-Jr.pdf

Thornthwaite, C.W., 1948. An approach toward a rational classification of climate. Geog. Rev. 38 (1), 55–94. https://doi.org/10.2307/210739

Turc, L. 1954. The water balance of soils: relationship between precipitations, evaporation and flow (In French: Le bilan d'eau des sols: relation entre les précipitations, l'évaporation et l'écoulement), Annales Agronomiques, Série A, 491-595.

Yokoo, Y., Sivapalan, M., Oki, T. 2008. Investigating the role of climate seasonality and landscape characteristics on mean annual and monthly water balances. J. Hydrol. 357 (255–269). https://doi.org/10.1016/j.jhydrol.2008.05.010

~~16~~12 Appendix: further details to justify our choice for the synchronicity index

There is no unique solution for choosing a measure of synchronicity between Precipitation and Potential Evaporation. In a previous paper (de Lavenne & Andréassian, 2018) we ~~had~~ presented a non-dimensional index (λ), defined as follows ~~see~~ (Eq. 8~~Eq. 1~~) ~~which had the desirable properties:~~,

$$\lambda = \frac{\sum_{m=1}^{12} min\left(P_{m,n} \cap, E_{0_{m,n}}\right)}{\sum_{m=1}^{12} max\left(P_{m,n} \cup, E_{0_{m,n}}\right)} \quad \textbf{Eq. 8}$$

A reviewer of this paper remarked that our interpretation of this index did not hold in extreme cases. Thus, we modified it in order to improve its interpretability~~and this index proved again to be adapted in this study~~. We ~~did however try~~also tried to replace it with simpler versions, and we would like to present these alternatives in order to save time and effort for those who would like to keep working on this topic.

The first simplification which was tested (called here $S1$) consisted in using directly the synchronous~~numerator of the λ index as~~ $P - E_0$ amount ~~follows~~:

$$~~S1_n~~ S1(n) = \sum_{m=1}^{12} min\left(P_{m,n} \cap, E_{0_{m,n}}\right) \quad \textbf{Eq. 9~~95~~}$$

$S1$ was an interesting solution because it yielded directly a value in [mm/y], without the need for rescaling, and it clearly represented the precipitation volume that was the most easily accessible to evaporation. In the linear regression, it did give very high average adjusted R^2 (world average of ~~0.70~~0.67, the same as for the solution retained). The reason why we did not consider this solution was that there was a correlation between $\Delta S1$ and ΔP for many catchments (average correlation of +0.58 over the 4122 catchments, reaching +0.74 over the Australian catchments), and introducing two correlated variables in a regression equation is clearly bad statistical practice.

To avoid this high correlation, we tested a ~~simplified version of the λ index~~normalization using annual precipitation, which we redimensionalized using the average interannual precipitation as in Eq. 10~~Eq. 10Eq. 6~~ below:

$$S2(n) = \frac{\sum_{m=1}^{12} min\left(P_{m,n} \cap, E_{0_{m,n}}\right)}{P_n} * \bar{P} \quad \textbf{Eq. 10~~106~~}$$

a mis en forme : Autoriser lignes veuves et orphelines

a mis en forme : Police :Cambria Math

The problem we found with $S2$ was that it yielded a constant value (equal to $\bar{P}$) for many arid catchments, where for most of the years $\frac{\sum_{m=1}^{12}\left(P_{m,n} \cap E_{0_{m,n}}\right)}{P_n} = 1$ because $P_{m,n} \ll E_{0_{m,n}}$.

We also tested a normalization using annual potential evaporation, which we redimensionalized using the average interannual potential evaporation as in Eq. 11 below:

$$S3(n) = \frac{\sum_{m=1}^{12} min\left(P_{m,n}, \cap E_{0_{m,n}}\right)}{E_{0_n}} * \overline{E_0} \qquad \text{Eq. 11}$$

But $S3$ behaved similarly as $S1$ (clearly because the $\frac{\overline{E_0}}{E_{0_n}}$ ratio is always close to 1), and the issue of having highly correlated values of $\Delta S3$ and ΔP reappeared.

This is why we finally opted for ~~a~~ combin~~ation of~~ing $S2$ and $S3$ using a geometric average (~~using the original λ index (which never reaches 1, and~~, which correlation with the annual P is low: -0.~~18~~ 10 on average), which w~~e~~as then redimensionalized using the average interannual precipitation.~~.~~ ~~Redimensionalizing λ was logically made by multiplying it by $\overline{\sum_{m=1}^{12}\left(P_{m,n} \cup E_{0_{m,n}}\right)}$, which is a constant value for each catchment and does not modify the correlation with P_n.~~ This yielded Λ_n, which has the desired dimension (mm/y), and was used throughout this paper.

$$\Lambda_n = \frac{\sum_{m=1}^{12} min\left(P_{m,n}, E_{0_{m,n}}\right) \left[\sum_{m=1}^{12}\left(P_{m,n} \cap E_{0_{m,n}}\right)\right]}{\sqrt{P_n E_{0_n}}} * \bar{P} \qquad \text{Eq.4}$$

a mis en forme : Non Surlignage

a mis en forme le tableau

a mis en forme : Police :10 pt

a mis en forme : Police :10 pt, Gras